MSEC2017-2731

DEVELOPMENT AND CHARACTERIZATIONS OF LIQUID BRIDGE BASED MICROSTEREOLITHOGRAPHY (LBMSL) SYSTEM

Yanfeng Lu

Mechanical Engineering, The University of Akron, Akron, OH, USA

Sumanth Kashyap

Mechanical Engineering, The University of Akron, Akron, OH, USA

Md. Omar Faruk Emon

Mechanical Engineering, The University of Akron, Akron, OH, USA

1

Jeongwoo Lee

Mechanical Engineering, The University of Akron, Akron, OH, USA

Jae-Won Choi*

Mechanical Engineering, The University of Akron, Akron, OH, USA

ABSTRACT

In this work, a novel liquid bridge microstereolithography (LBMSL) was proposed and developed. The liquid bridge was first introduced into the MSL process by replacing the vat, allowing the entire fabrication process to occur within the liquid bridge. The liquid bridge was studied theoretically and experimentally in order to obtain the stable equilibrium shape and the relationship between the height and the volume of the liquid bridge. Using the LBMSL process, the fabrication layer thickness of 0.5 µm was reached. This could not be easily achieved in the vat-based MSL due to the oxygen inhibition to the photopolymer. Fabrication of a photopolymer with a viscosity of 3000 cP was tested and significant results were obtained. Compared with the vat-based MSL, the material consumption in LBMSL was reduced and the fabrication time was improved greatly, in particular, when using higher viscous materials.

INTRODUCTION

Vat-based microstereolithography (MSL) is an attractive freeform 3D micro-fabrication technology, capable of fabricating complex 3D microstructures in a layer-by-layer fashion, in particular on micro-scale level. Two methods, top-down and bottom-up projection systems have been used commonly by researchers [1].

In the top-down projection system, a new resin surface is refreshed by immersing a substrate deeper into the resin vat so that the fresh resin flows on top of the previously fabricated layer. Although the configuration of this top-down system is relatively simple, time is wasted for steps required to refresh the surface and highly viscous photopolymers are difficult to be used. In addition, oxygen near the photopolymer surface inhibited photopolymerization, resulting in poor curing [2], which is significant in micron-size layers. To overcome these drawbacks, a glass window can be used to confine the resin surface [3]. In contrast, the bottom-up projection system, refreshing the resin surface is fast since the substrate is moved up and a fresh resin is supplied from the bottom [4]. It has the advantages of multi-material fabrication, faster fabrication, comparatively less amount of material used and lower oxygen inhibition effects, while the configuration is complex. Moreover, a vat is necessary to hold a photopolymer for both methods of MSL, which needs considerable amount of a material even just to fabricate a tiny structure.

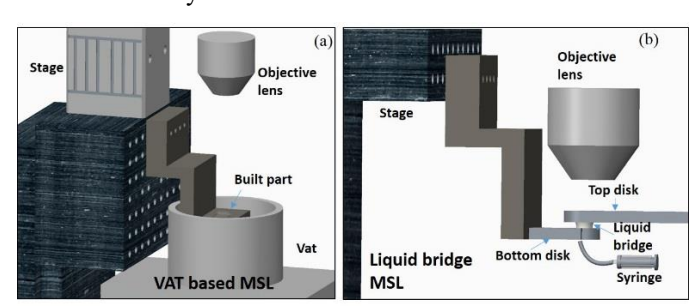


Figure 1. Schematic of (a) vat-based MSL and (b) LBMSL.

In this endeavor, a new layer-stacking mechanism using an equilibrium quasi-static liquid bridge has been proposed by taking advantages of both top-down and bottom-up projection

processes [5-7]. A liquid bridge is formed between two round parallel coaxial disks with the same diameter to replace the vat in vat-based MSL, as shown in Figure 1. The following sections describe experimental and results in more detail.

EXPERIMENTAL

The entire system consisted of several subsystems [1, 8]. Light emission subsystem includes a mercury lamp and optical fiber (OmniCureTM S2000, Lumen Dynamics, Canada), with an output of 200 W and a filtered wavelength of 365 nm to deliver the light from the lamp to a collimating lens set. Light delivery subsystem is composed of a prism to steer the light path from the optical fiber to DMDTM (Digital Micromirror Device, Texas Instrument, US), which is a pattern generator. A relay lens and reflecting mirror were used to deliver the patterned light from the DMD to a projection lens (20 mm in focal length and 0.13 in numerical aperture (N. A.)). Stacking layers was realized by a high-precision Z stage (Aerotech, PA, US) with a resolution of 500 nm. More detail information on the system used in this work can be found in [1, 8]. A platform for the liquid bridge includes two parallel coaxial disks with the same diameter, a top disk holder, a bottom disk holder, and syringe. (Figure 2). A channel was created through the bottom disk letting the syringe tip to deliver the material. The bottom disk holder along with the bottom disk was mounted on the Z stage to move up and down.

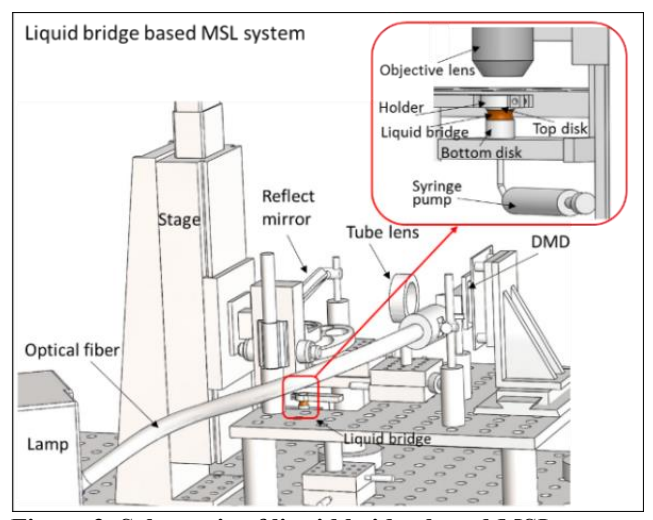


Figure 2. Schematic of liquid bridge based MSL system.

The fabrication principle and process were similar to the vatbased MSL, including the model and cross sectional images preparation. The difference was that a liquid bridge was adopted to replace the vat in the vat-based MSL. Figure 3 simply depicted the entire fabrication process. Before fabrication, the top and bottom disks were in contact each other, and then the bottom disk was moved down for an exact one layer thickness distance. A liquid material was fed between two disks by the syringe pump using a predetermined volume to form a proper liquid bridge. After the liquid bridge was formed, a short settling time, dependent on the viscosity of the material, was given to allow the liquid bridge to be stabilized. Then the first layer fabrication could be started. Since the surface tension of the top disk was lower than the bottom disk, the adhesion force between the bottom disk and the built layer was much greater than that between the top disk and the built layer. Therefore, the built layer was detached from the top disk and moved down with the bottom disk for one layer thickness distance. As the built layer was detached from the top disk, a vacuum area was generated. The suction force produced by the vacuum pulled the material in, filling the gap rapidly, even though it was a high viscosity material. After the settling time was given to stabilize the liquid bridge, the next layer fabrication was started. By repeating this process, a 3D structure can be fabricated by stacking all the layers. After fabrication, the remaining material would be drawn back by the syringe and recycled. Cleaning and post-processing are necessary in this fabrication method.

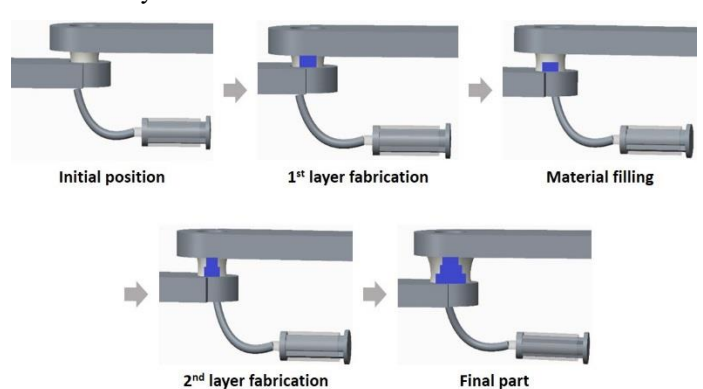


Figure 3. Schematic of fabrication process using LBMSL method.

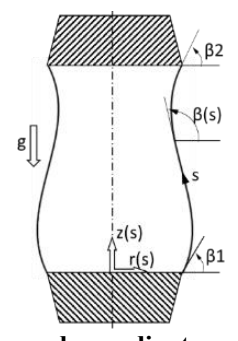


Figure 4. Geometry and coordinate system for the liquid bridge model.

For a constant height, a liquid bridge profile can be varied from a slender shape to a plump shape depending on the material volume [9]. In the fabrication process, the effective fabrication space and the stability should be taken into account since the entire fabrication occurred within the liquid bridge and the vibration and perturbation caused by the moving stage and material feeding were inevitable. In addition, the bottom disk had to be moved down to a pre-determined distance after each layer of fabrication to fill the material for the next layer of fabrication and also to maintain the stable liquid bridge profile. The

relationship between the volume and the height was important for the material feeding. A mathematical model was necessary to seek the most stable liquid bridge profile and the relationship between the volume and height.

The liquid bridge has been mathematically modeled and the profile of the bridge along the vertical direction can be computationally calculated [5]. A key point for the suggested stacking mechanism is how to maintain the desired area and thickness of the liquid bridge at the top surface that also provides a refreshed resin layer. As a result, the material amount supplied as the distance between the disks increases should be obtained. This can be simulated with the following Young-Laplace equations [5, 10] to obtain the profile of the bridge and the simulation results will be compared with experiments (Figure 4):

$$r''(s) = -z'(s)\beta'(s) \tag{1}$$

$$z''(s) = r'(s)\beta'(s) \tag{2}$$

$$\beta'(s) = -z(s) + \frac{\Delta P}{\sqrt{\rho g \gamma_p}} - \frac{z'(s)}{r(s)}$$
(3)

where, s is the arc length of the free surface, r(s) is the radius of the bridge, z(s) is the height from the substrate, $\beta(s)$ is the angle of between the r axis and the tangent of the arc length s, ΔP is the Laplace pressure difference between the inside and outside of the liquid, ρ is the density of the liquid, g is the acceleration of gravity, and γ_p is the surface tension of the photopolymer. These equations can be solved with several boundary conditions $r(0)=r_0$, $r'(0)=cos\theta$, z(0)=0, $z'(0)=sin\theta$, and $\beta(0)=\theta$. And thus, we can calculate a volume to be dispensed by obtaining a new profile of the bridge with the modified parameters such as h while fixing the radius. MATLAB was adopted to integrate the equations. The volume of the liquid corresponding to each $\beta 1$ can be calculated by:

$$V = \pi \int_0^s r^2(s)z'(s)ds \tag{4}$$

RESULTS AND DISCUSSION

In this work, monomer combination propoxylated (5.5) glyceryl triacrylate (CD9021, Sartomer) and 1, 6-hexanediol diacrylate (HDDA, Aldrich) (70w/30w) was applied to the mathematical model to obtain the equilibrium shape and the volume for each β 1 of the liquid bridge. The parameters needed in this integration were: ρ =1×1.16³ kg/m³, σ =0.035 N/m, and g=9.8 m/s². The equilibrium shape and the volume was achieved from the mathematical model with the constant height of 3 mm and a varying β 1 from 70° to 120° with intervals of 10°.

Liquid bridge experiments were conducted to verify the mathematical model. The liquid bridge was formed between two disks and the material was fed from the center of the bottom disk by a precise pump syringe (Figure 1(b)). By maintaining a constant height of 3 mm and changing the volume of the material, liquid bridge profiles were captured by a camera. The

experimental results were then compared with the mathematical results (Figure 5).

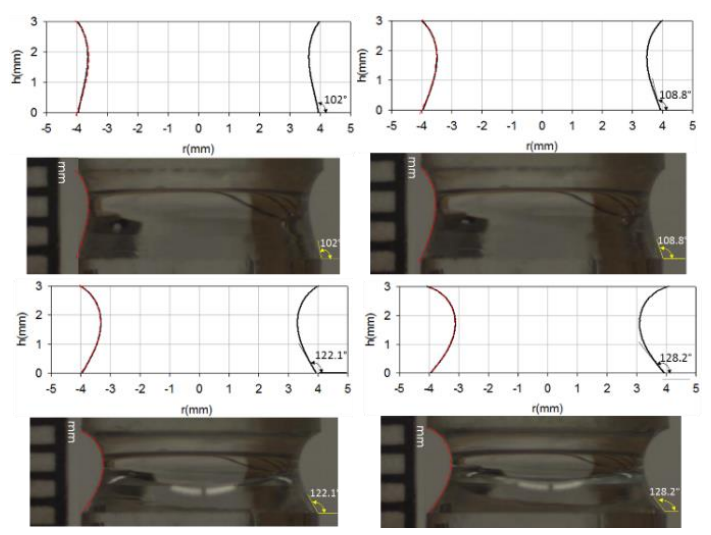


Figure 5. The equilibrium shapes of liquid bridge for CD9021/HDDA (70w/30w) from the experiments and mathematical model with different $\beta1$.

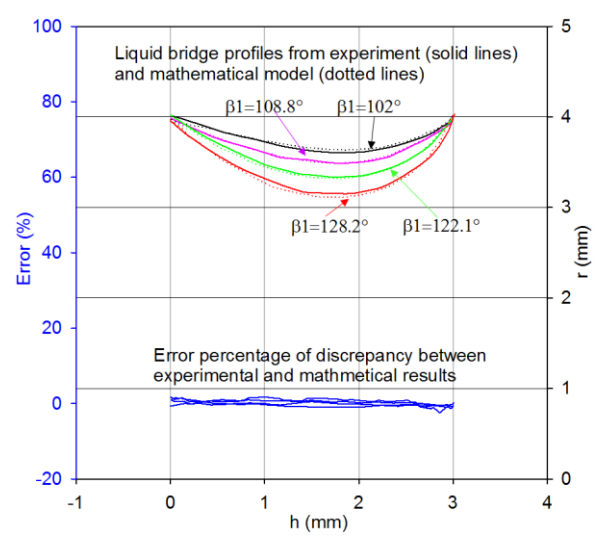


Figure 6. The comparison of liquid bridge profiles from the experimental and mathematical model results.

The liquid bridge profiles obtained from the experiments and mathematical model have a good agreement (Figure 6). Therefore, the mathematical model can be applied to photopolymers with similar properties to achieve the stable equilibrium shape and the relationship between the height and the volume.

In conventional vat-based MSL system, since the oxygen in the air was in direct contact with the polymer surface during the fabrication process, the oxygen inhibition is an obstacle to obtain the fabrication layer thickness down to 1 μ m or less [11]. However, in LBMSL system, the top disk separated the top surface of the photopolymer from the air, and the oxygen inhibition was reduced greatly [12]. Figure 7 is a post array

including 4 sections with a varying layer thickness of 0.5 $\mu m, 1$ $\mu m, 10$ $\mu m,$ and 20 μm for each section from top to bottom for each single post. The layer thickness of 0.5 μm was first obtained due to the reduced effects of oxygen inhibition in LBMSL process.

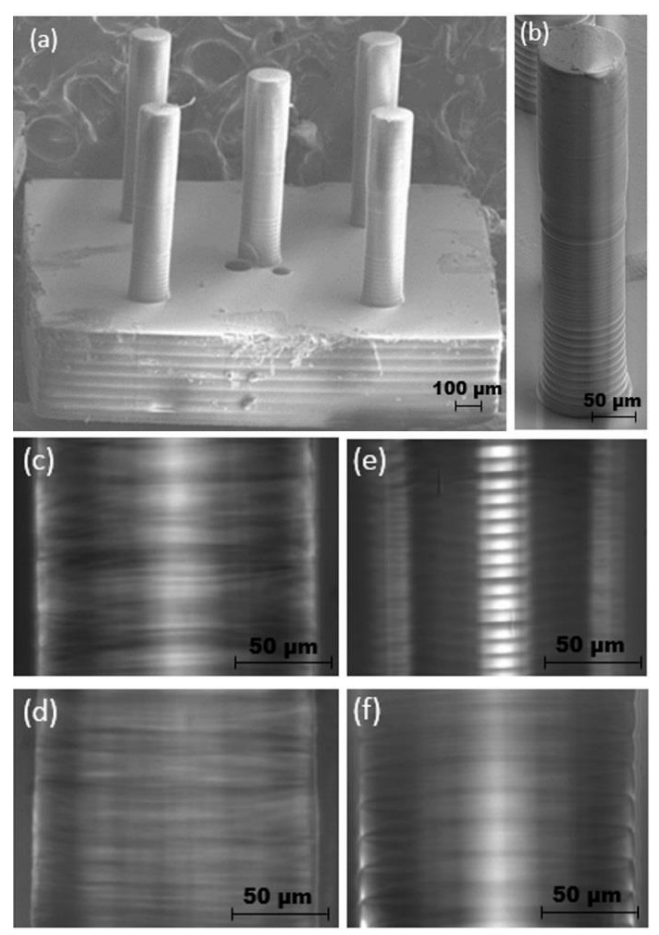


Figure 7. Posts with the layer thickness. (a) SEM image of one post, magnified microscopy images of the part with (c) $20 \mu m$, (d) $10 \mu m$, (e) $1 \mu m$ and (f) $0.5 \mu m$.

As discussed in previous section, the fabrication time for the vat-based MSL was considerable due to the slow material refreshing process for each layer, especially for a high viscous material (typically more than 200 cP [13]). For LBMSL, however, after one layer fabrication, the built part was moved down with the bottom disk and there was a vacuum area formed between the built part and the top disk. The suction force generated by the vacuum can pull the material to fill the gap fast followed by the next layer fabrication. Figure 8 (a) and (b) are spring structures fabricated by the vat-based MSL and LBMSL using the material of dimethacrylate (SR150) with the viscosity of 700 cP at 25 °C. And Figure 8 (c) and (d) were springs fabricated by the vat-based MSL and LBMSL using the material Acrylated polyester oligomer (CN293, Sartomer)/HDDA (90w/10w) with the viscosity of 3200 cP at 25 °C.

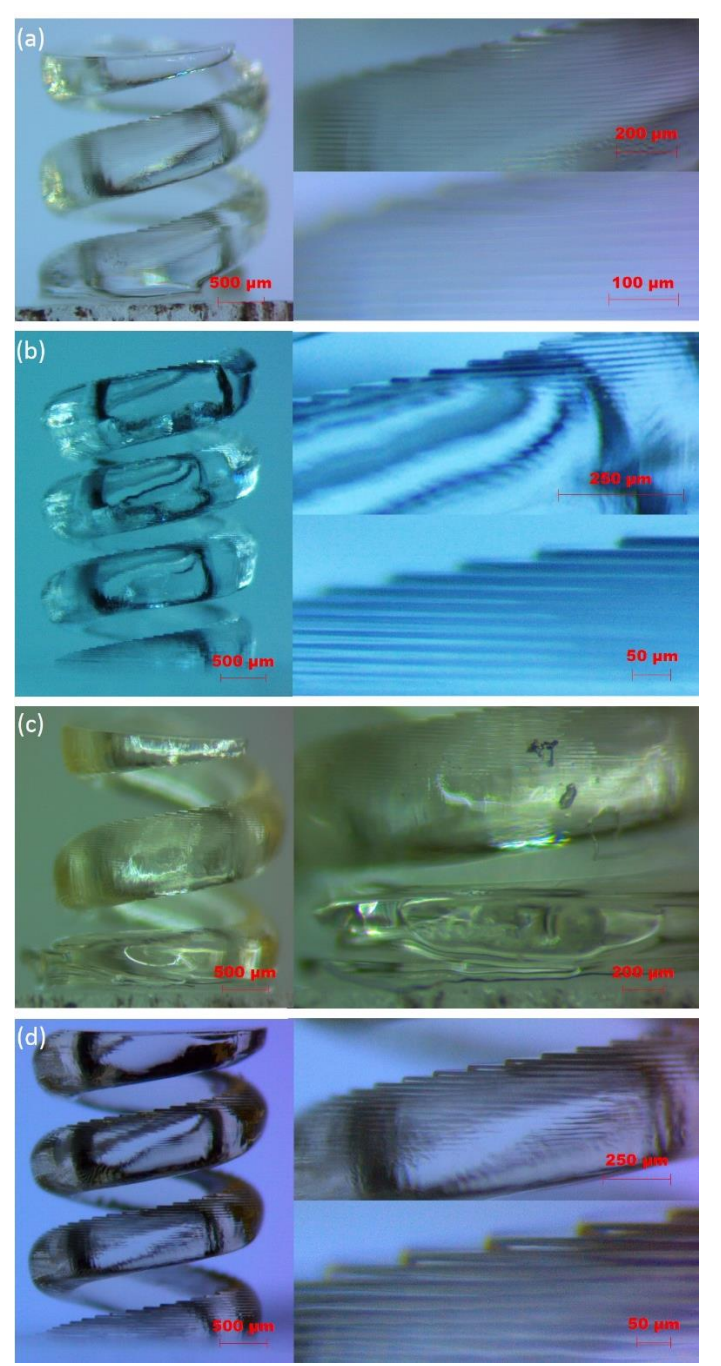


Figure 8. Spring structures fabricated by (a) vat-based MSL process with the fabrication time of 3.74 h, (b) liquid bridge-based MSL process with the fabrication time of 0.87 h, (c) vat-based MSL process with the fabrication time of 5.4 h, and (d) liquid bridge-based MSL process with the fabrication time of 1.07 h.

From the fabrication results, when using SR150 with the viscosity of 700 cP, the fabrication time for the vat-based MSL was 3.8 times more than the LBMSL, this value increased to 5 when using a higher viscosity material, CN293/HDDA (90w/10w). Comparing the fabrication parameters, the settling

time was increased greatly when using a higher viscous material in vat-based MSL, while no big change was noticed for settling time for LBMSL. Therefore, LBMSL exhibited a potential for high viscosity material fabrication, which can broaden the material selection significantly for the MSL process.

Figure 9 shows microneedle structures fabricated by the LBMSL process with different layer thickness. The material was CD9021/HDDA (70w/30w), with DMPA (1 w%) and Tinuvin $327^{\$}$ (0.1 w% [14]) as the photoinitiator and light absorber, respectively.

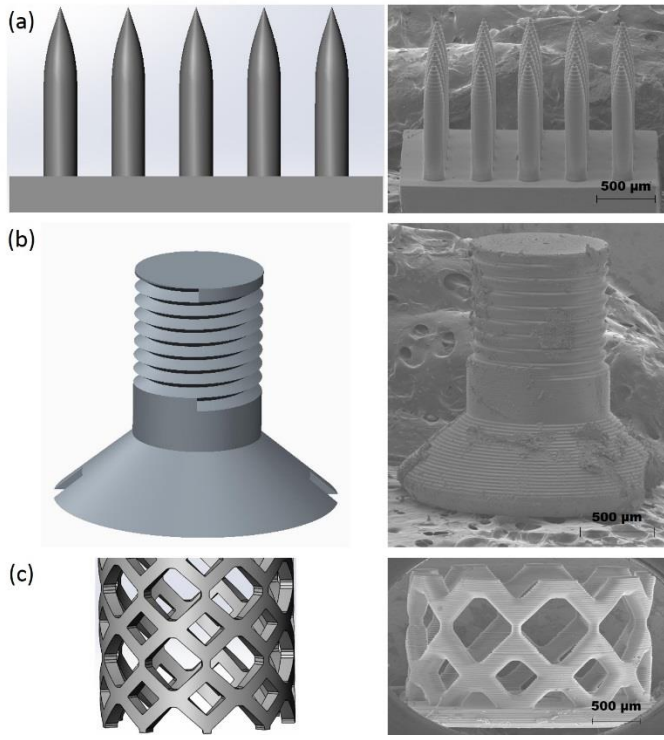


Figure 9. Fabrication examples by the LBMSL process: (a) Microneedle array [15], with the layer thickness of 30 um, (b) screw and stent with the layer thickness of 20 um. In each picture, the left was the model.

CONCLUSIONS

The novel LBMSL process showed advantages in terms of fabrication speed, high viscosity material fabrication, the submicron layer thickness, and lower material consumption. The advanced process improved the fabrication capacity of MSL and could be used for numerous applications. The liquid bridge was mathematically modeled and the profile of the bridge was simulated. A series of experiments to verify the mathematic model were conducted and evaluated. The developed model had a good agreement with the experimental results. Using the developed process several micro-structures were fabricated to demonstrate the fabrication capacity of LBMSL. It is believed that the developed process could be a potential 3D microfabrication means with high resolution using highly viscose

materials which can't be easily used in the conventional MSL processes.

ACKNOWLEDGMENTS

This work was supported by The University of Akron FRC Grant and partially supported by the National Science Foundation under grant no. CMMI MME-1636118.

REFERENCES

- [1] Choi, J.W., Lu, Y., and Wicker, R.B., 2015, Projection microstereolithography as a micro-additive manufacturing technology, Additive Manufacturing: Innovations, Advances, and Applications (CRC Press).
- [2] Klang, J.A., 2008, "Radiation curable hyperbranched polyester acrylates," Sartomer Company, Inc., Exton, PA (http://www.sartomer.com/TechLit/5064.pdf).
- [3] Takagi, T. and Nakajima, N., 1993, "Photoforming applied to fine machining," *In 4th International Symposium on Micro Machine and Human Science* (MHS'93).
- [4] Zhou, C., Chen, Y., Yang, Z., and Khoshnevis, B., 2013, "Digital material fabrication using mask-image-projection-based stereolithography," *Rapid Prototyping Journal*, *Vol.* 19, pp. 153.
- [5] Qian, B. and Breuer, K.S., 2011, "The motion, stability and breakup of a stretching liquid bridge with a receding contact line," *Journal Fluid Mechanics*, *Vol.* 666, pp. 554.
- [6] Chen, H., Tang, T., and Amirfazli, A., 2013, "Modeling liquid bridge between surfaces with contact angle hysteresis," *Langmuir*, *Vol.* 29, pp. 3310.
- [7] Chen, H., Tang, T., and Amirfazli, A., 2014, "Liquid transfer mechanism between two surfaces and the role of contact angles," *Soft Matter, Vol. 10*, pp. 2503.
- [8] Choi, J.W., Ha, Y.M., Lee, S.H., and Choi, K.H., 2006, "Design of microstereolithography system based on dynamic image projection for fabrication of threedimensional microstructures," *Journal of mechanical* science and technology, Vol. 20, pp. 2094.
- [9] Slobozhanin, L.A. and Perales, J. M., 1993, "Stability of liquid bridges between equal disks in an axial gravity field," *Physics of Fluids A: Fluid Dynamics, Vol. 5*, pp.1305.
- [10] Lautrup, B., 2011, Physics of continuous matter, 2nd Edition: Exotic and everyday phenomena in the macroscopic world (CRC Press).
- [11] Ku, S-B. and Gerald, E.E., 1997, "Oxygen inhibition of photosynthesis I. Temperature dependence and relation to O2/CO2 solubility ratio," *Plant Physiology*, *Vol.* 59, pp. 986.
- [12] Ligon, S.C., Husar, B., Wutzel, H., Holman, R., and Liska, R., 2013, "Strategies to reduce oxygen inhibition in photoinduced polymerization," *Chemical Reviews*, Vol. 114, pp. 557.
- [13] Choi, J.W., Wicker, R., Lee, S.H., Choi, K.H., Ha, C.S., and Chung, I., 2009a, "Fabrication of 3D biocompatible/biodegradable micro-scaffolds using dynamic mask projection microstereolithography," *Journal of Materials Processing Technology*, Vol. 209, pp. 5494.

- [14] Choi, J.W., Wicker, R.B., Cho, S.H., Ha, C.S., and Lee, S.H., 2009b, "Cure depth control for complex 3D microstructure fabrication in dynamic mask projection microstereolithography," *Rapid Prototyping Journal*, *Vol.* 15, pp. 59.
- [15] Lu, Y., Mantha, S.N., Crowder, D.C., Chinchilla, S., Shah, K.N., Yun, Y.H., Wicker, R.B., and Choi, J.W., 2015, "Microstereolithography and characterization of poly (propylene fumarate)-based drug-loaded microneedle arrays," *Biofabrication*, *Vol.* 7, pp. 045001.